# CHAPTER 9

# PLANETARY MAGNETOSPHERES

Frances Bagenal
Space Physics Group
The Blackett Laboratory
Imperial College of Science and Technology
London SW7 2BZ

Of the six planets visited by spacecraft, four (Mercury, Earth, Jupiter and Saturn) are known to have internally-generated magnetic fields. By the end of the decade we shall know if Uranus and Neptune are similarly endowed. The regions of space influenced by these planetary magnetic fields range in size from just a layer around the planet in the case of Mercury to the giant Jovian magnetosphere which occupies a volume at least 300 times the volume of the sun. Exploration of the plasma environments near these magnetised planets and studies of their interaction with the solar wind has led to the development of a comparative theory of magnetospheres. Although the word magnetosphere strictly implies that the central body has an intrinsic magnetic field, there are several objects in the solar system which are not magnetised but nevertheless strongly interact with the solar wind. I shall therefore stretch the definition of magnetosphere to include them. I shall also consider some of the satellites that are embedded in a planetary magnetosphere and their interaction with the surrounding plasma flow.

The first section of this chapter is an outline of a comparative theory of magnetospheres. The second section is a survey of the magnetospheres of the solar system starting with the innermost planet Mercury and working radially outwards to Pluto, considering how each case fits into the generalised theory. Comparative studies of magnetospheres have only recently been developed. Since the ground work was laid down by Siscoe(1979) there have been considerable changes in our understanding of the magnetospheres of Venus, Jupiter and Saturn. Recent reviews, taking rather different approaches to the subject, are given by Stern and Ness(1982), Vasyliunas(1983a) and McNutt(1984).

## 9.1 COMPARATIVE THEORY OF MAGNETOSPHERES.

I shall begin with a simple description of the different ways in which objects interact with a flowing plasma. The nature of the interaction depends on the characteristics of the central body (e.g. its electrical conductivity, the presence of an atmosphere or whether the object has an internally-generated magnetic field) and the properties of the external

plasma flow (e.g. the sonic and Alfvenic Mach numbers of the flow). Then I consider the possible sources of plasma and the dominant plasma motions in the case where the central object has a magnetic field of sufficient strength to form a magnetosphere.

### 9.1.1. Obstacles in a flowing plasma

By the time plasma from the sun reaches the planets its kinetic energy is largely bulk motion (i.e. the flow is supersonic) and, as the interplanetary magnetic field (IMF) is weak, the solar wind is super-Alfvenic (see Chapter 8). The fact that the solar wind is supersonic* means that generally there is a bow shock upstream of the obstacle. The plasma is slowed down and heated as it passes through the shock and hence the flow around the obstacle is then sub- or trans-sonic. In contrast to the solar wind, plasma flows in planetary magnetospheres span wide ranges of sonic and Alfvenic Mach numbers, a consideration that must be kept in mind when comparing the plasma interactions of different planetary satellites.

With regard to the characteristics of the obstacle, it is convenient to consider first the two extreme situations where the object is taken to either a perfect insulator or a perfect conductor. It is then necessary to consider the effects of finite conductivity since planetary bodies probably have effective conductivities in a range between these extremes.

#### (i) Non-conducting object

A magnetic field diffuses through an object with a timescale $\tau_d \sim \mu_0 \sigma L^2$, where L is the size and $\sigma$ the electrical conductivity of the body. If this diffusive timescale is much less than the timescale for changes in the ambient magnetic field then the field passes through the body largely unperturbed. For a magnetic field 'frozen' into a plasma flowing at characteristic speed V the object sees the field change over the convective timescale $\tau_c \sim L/V$. Hence the magnetic interaction is weak for a non-conducting body with low magnetic Reynolds number ($R_m = \tau_d/\tau_c = \mu_o \sigma VL \ll 1$).

In the case of a supersonic flow, although the magnetic field readily diffuses through the non-conducting body the plasma particles obviously cannot penetrate the body and are therefore absorbed. Because the flowing plasma is absorbed on the upstream surface there is a cavity behind the object and a wake is formed downstream as the plasma expands into the low pressure region (Figure 1a).

For subsonic flow, the interaction depends on whether the plasma is dominated by the particles' kinetic pressure or the magnetic pressure. Thus for a plasma where the ratio $\beta=(nkT)/(B^2/2\mu_o)$ is small the magnetic field controls the flow and the plasma is absorbed by the non-conductor. For high-$\beta$ plasmas the subsonic flow is deflected around the object in the smooth, laminar flow of hydrodynamics, taking the weak magnetic field with it.

When there is a relative motion $\underline{V}'$ between a magnetised plasma and a conducting body the Lorentz electric field $\underline{E} = -\underline{V}' \times \underline{B}$ drives a current $\underline{J}=\sigma\underline{E}$ in the object (Figure 1b). The current in the body in turn produces a perturbation in the background magnetic field. Since the magnetised plasma is highly anisotropic (with $\sigma_{\parallel} \gg\gg \sigma_{\perp}$ ) the current is carried away from the flanks of the object along the magnetic field.

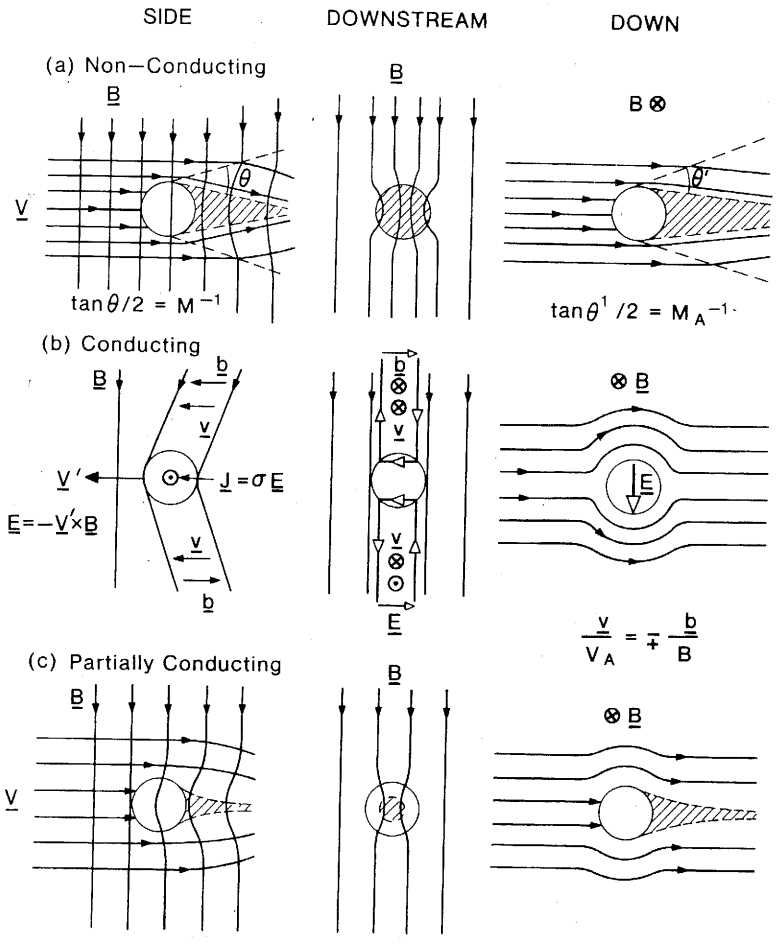


Figure 9.1 The interaction of a magnetised plasma with a (a)non-conducting; (b) conducting; (c) partially-conducting object. The hatching indicates the region of low density in the object's wake.

In the magnetohydrodynamic (MHD) regime the plasma flow is coupled to the magnetic field and hence the plasma flow is also perturbed by the conducting body. In the case of a perfect conductor (i.e. $R_m \gg\gg 1$) the resulting motion of the plasma in the tube of magneti c flux that intersects the body exactly matches the motion of the conductor. The surrounding plasma is then deflected around the body in a manner similar to incompressible hydrodynamic flow around a cylinder with essentially no wake downstream (Drell et al.,1965). The perturbations in the magnetic field ($\underline{b}$) and plasma flow ($\underline{v}$) are an Alfven wave which propagates along the ambient magnetic field with a characteristic speed $V_A=B/\sqrt{(\mu_o \rho)}$ and satisfies the Alfven relation $\underline{v}/V_A=+\underline{b}/B$ (where the sign corresponds to

propagation parallel or anti-parallel to the ambient magnetic field). One can consider these Alfven waves to be carrying the field-aligned currents.

(iii) Partially- conducting object

When the object has a finite conductivity the flow perturbation is insufficient to allow all of the surrounding plasma to flow around the body and hence some is absorbed (Figure 1c). At the same time a finite amount of the kinetic energy of the plasma flow is dissipated in the body as Joule heating. Thus finite resistivity leads to deceleration of the plasma flow near the object and the magnetic field being "hung-up" in the stagnant flow. Since the magnetic field far from the object continues to be convected in the unperturbed flow the magnetic field lines become bent or "draped" over the object to form a magnetic tail or wake downstream.

(iv) Object with an atmosphere

On the dayside of all objects having an atmosphere the sun's ultraviolet emissions ionise some of the neutral atoms. For objects that are embedded in a dense plasma, ionisation by particle impact may also be significant. In any case, the degree of ionisation determines the conductivity of the upper atmosphere (ionosphere) and thus affects the nature of the interaction of the object with the plasma in which it is immersed. In the case of a dense ionosphere ($\sigma \to \infty$) the solar wind magnetic field is excluded and the flow is diverted around the flanks of the body. The boundary between the ionosphere and the surrounding

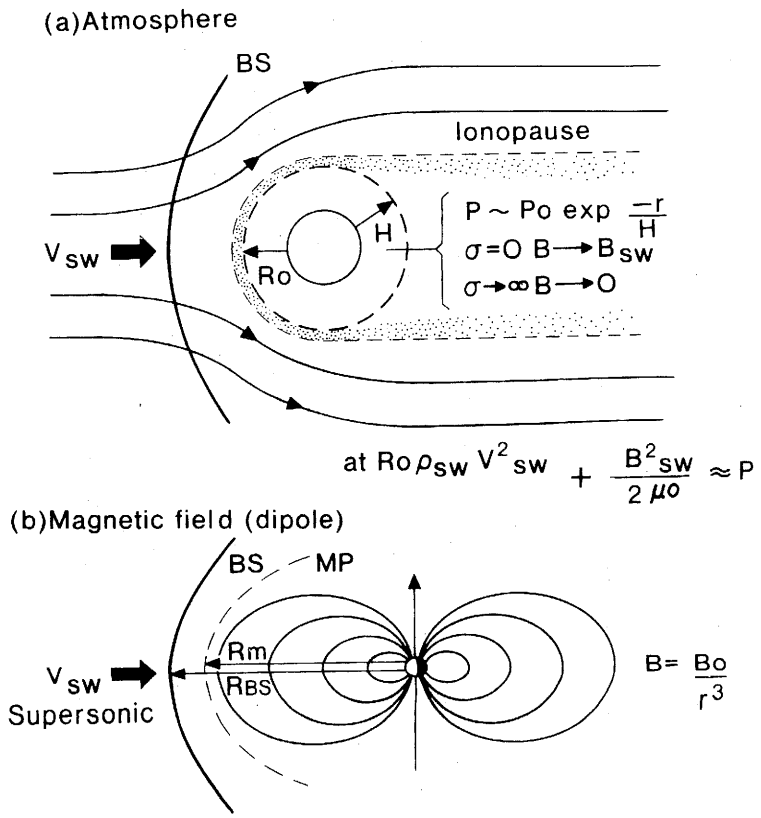


Figure 9.2 The interaction of a magnetised plasma with an object posessing (a) an atmosphere of surface pressure $P_o$ and a scale height H; (b) a magnetic field. The bowshock(BS) and magnetopause(MP) are shown.

magnetic and ram pressure of the external plasma is balanced by the particle pressure (P) in the ionosphere (Figure 2a). When the ionisation is weak ($\sigma \to 0$) the magnetic field and plasma flow are dragged through the resistive ionosphere causing a substantial downstream wake. We must further consider the consequences of the ionisation of any neutral material extending out into the streaming plasma. On ionisation the particle 'sees' the Lorentz electric field due to its motion relative to the plasma and is accelerated up to the ambient flow. The momentum gained by the newly-created ions comes from the surrounding plasma which correspondingly loses momentum. This effect is called 'mass loading' and contributes to the draping of field lines over an object with a substantial atmosphere (e.g. comets, Venus and Titan).

(v) Magnetised object

Well before Biermann(1957) provided cometary evidence of a persistent solar wind, Chapman and Ferraro (1931) considered how a strongly magnetised body (the Earth) would deflect a flow of particles from the Sun. They proposed that a dipolar magnetic field (of strength $B_0$ at the planet's equatorial radius $R_p$) would stand off the flow to a distance $R_{cf}$ where the ram pressure of the flow balances the Maxwell stress of the magnetic field

$$\rho_{sw} V_{sw}^2 = \tfrac{1}{2} \frac{B_0^2}{\mu_0} \left( \frac{R_p}{R_{cf}} \right)^6 . \qquad (9.1)$$

Hence

$$\frac{R_{cf}}{R_p} = \left( \frac{\tfrac{1}{2} B_0^2}{\mu_o \rho_{sw} V_{sw}^2} \right)^{1/6} . \qquad (9.2)$$

This not only assumes that $B_{sw} \ll B_0 (R_p/R_{cf})^3$ (which is generally reasonable but also that the particle pressure inside the magnetosphere is negligible. In reality, the observed stand-off distances, $R_m$ are between 1 and 2 times $R_{cf}$.

Thus, to first approximation, the magnetic field of the object deflects the plasma flow around it, carving out a cavity in the solar wind. The boundary between the magnetosphere and the solar wind is called the magnetopause (MP) and the layer of deflected solar wind flow behind the bowshock(BS) is called the magnetosheath. The solar wind generally pulls out part of the planetary magnetic field into a long cylindrical magnetotail, extending far downstream behind the planet.

9.1.2. Plasma Sources

It is rather misleading to describe the region dominated by a planetary magnetic field as an empty cavity from which the solar wind is excluded. Magnetospheres contain considerable amounts of plasma which have "leaked

in" from various sources (Figure 3). Firstly, the magnetopause is not entirely "plasma-tight". Whenever the IMF has a component anti-parallel to the planetary field, magnetic reconnection is likely to occur and solar wind plasma will leak into the magnetosphere across the magnetopause (see Chapter 5). Secondly, although ionospheric plasma is generally cold and gravitationally bound to the planet, a small fraction has sufficient energy to escape up magnetic field lines and into the magnetosphere. Thirdly, the interaction of magnetospheric plasma with any natural satellites that are embedded in the magnetosphere can generate significant quantities of plasma. Possible mechanisms for these satellite sources are (a)ionisation of the outermost layers of any satellite atmosphere; (b) energetic particle sputtering of the satellite surface producing less energetic ions directly or an extensive cloud of neutral atoms which are eventually ionised far from the satellite.

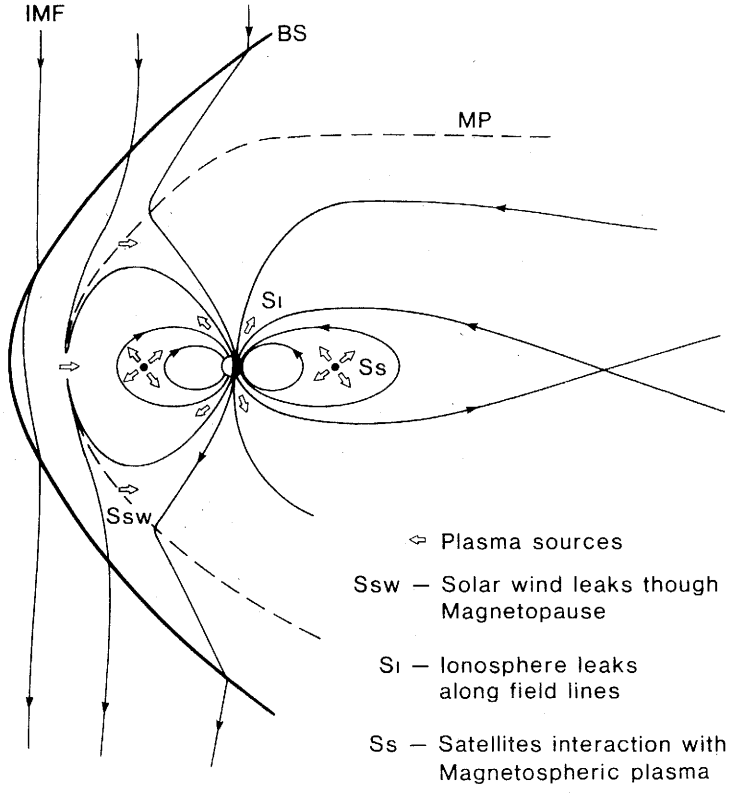


Figure 9.3 Sources of magnetospheric plasma.

### 9.1.3 Magnetospheric Flows

The two largest sources of momentum in planetary magnetospheres are the planet's rotation and the solar wind. The nature of any large scale plasma circulation (often called convection) in the magnetosphere depends on which momentum source is tapped. For magnetospheric plasma to rotate with the central body there are two basic requirements: (i) the planet's neutral atmosphere must corotate with the planet: (ii) the neutral atmosphere must be closely coupled to the ionosphere by collisions (i.e. the electrical conductivity of the ionosphere perpendicular to the field, $\sigma_\perp$ is large). In a corotating ionosphere (with velocity $\underline{V}^i$) any perpendicular (horizontal) currents are given by

Just above the ionosphere the perpendicular conductivity in the (collision-free) magnetosphere $\sigma_{\perp}^{m}$ is essentially zero. Thus

$$\underline{J}_{\perp}^{m} = \sigma_{\perp}^{m}(\underline{E}^{m} + \underline{V}^{m} \times \underline{B}) = 0 \qquad (9.4)$$

and

$$\underline{E}^{m} = - \underline{V}^{m} \times \underline{B} \quad . \qquad (9.5)$$

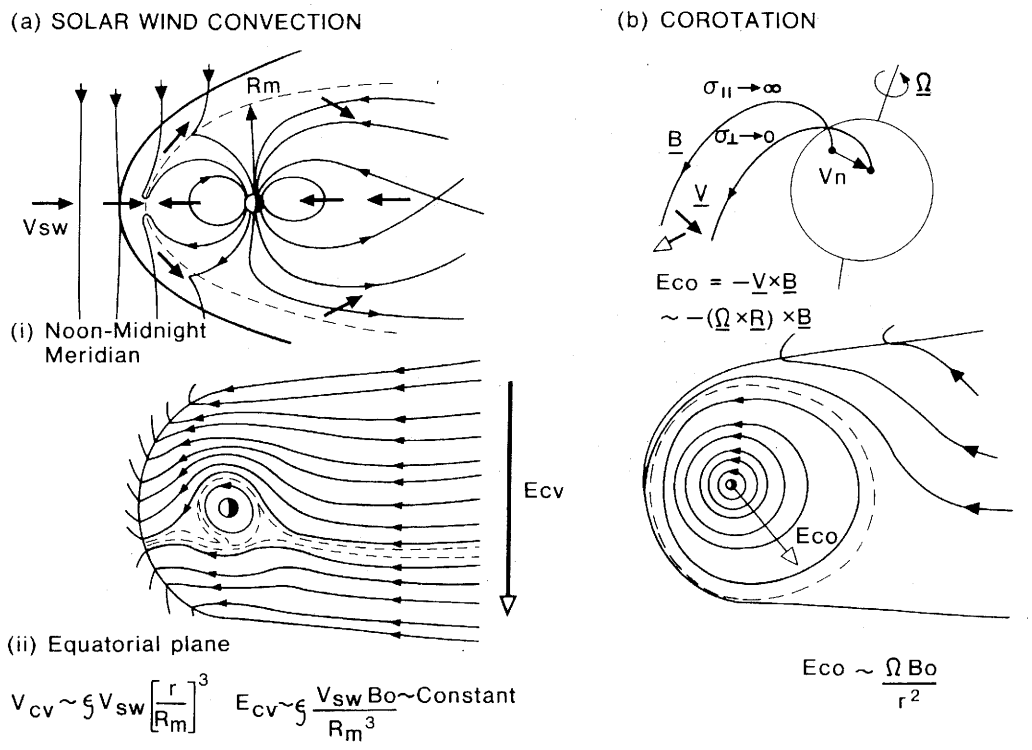


Figure 9.4 Large scale magnetospheric circulation driven by (a) the solar wind; (b) planetary rotation. The magnetic field directions are given corresponding to (a) Earth and (b) Jupiter.

Because the plasma particles are far more mobile in the direction of the local magnetic field the parallel conductivity, $\sigma_{\parallel}^{m}$ is large and the field lines can be considered to be equipotentials. Thus the electric field in the magnetosphere can be mapped into the ionosphere. Since the ionosphere is relatively thin the electric field $E^m$ obtained by evaluating (9.5) just above the ionosphere is the same as $E^i$. Substituting for $\underline{E}$ in (9.3) gives

$$\underline{J}_{\perp}^{i} = \sigma_{\perp}^{i}(\underline{V}^{i} - \underline{V}^{m}) \times \underline{B} \quad . \qquad (9.6)$$

The condition for corotation of the magnetospheric plasma is that $J^i/\sigma^i$ is sufficiently small that

$$\underline{V}^m = \underline{V}^i = \underline{\Omega} \times \underline{r} \quad . \tag{9.7}$$

For a dipolar magnetic field the corotational electric field is therefore radial with magnitude $E_{co} \sim \Omega B_0/r^2$ (Figure 4b). It is clear that large magnetospheric conductivities facilitate corotation. The large $\sigma^m$ also means that any currents in the magnetosphere ($J^m$) that result from mechanical stresses on the plasma (due to the solar wind interaction, for example) are directly coupled by field-aligned (Birkeland) currents to the ionosphere (discussed in Chapter 2). The ionospheric current density $\underline{J}^i$ is therefore proportional to $\underline{J}^m$ which is governed by the momentum equation in the magnetosphere

$$\rho \frac{d\underline{V}}{dt} + \nabla P = \underline{J}^m \times \underline{B} \quad . \tag{9.8}$$

Thus corotation breaks down when mechanical stresses on the magnetospheric plasma drive ionospheric currents which are sufficiently large that $J^i/\sigma^i$ becomes significant.

Where the magnetospheric plasma may be coupled to the planet's rotation via the ionosphere, the momentum of the solar wind is harnessed by processes occurring near the magnetopause. Although theories of a viscous drag between the solar wind and magnetospheric plasma rivalled theories of magnetic reconnection for many years, there is now evidence that the merging of the IMF with the planetary field on the dayside magnetopause is the dominant coupling process. The resulting convection pattern is caused by the reconnected magnetospheric flux tubes being pulled by the solar wind over the poles and back into an extended magnetotail (Figure 4a). The plasma then drifts towards the equatorial plane and eventually returns in a sunward flow to the dayside magnetopause. Cowley has described in Chapter 5 how the reconnection rate can be considered to be equivalent to an electric field, $E_{cv}$ which is assumed to be roughly constant with time

$$\underline{E}_{cv} = - \underline{V}_{cv} \times \underline{B} \sim \text{constant} \quad , \tag{9.9}$$

where $V_{cv}$ is the corresponding convection speed. $V_{cv}$ can then be estimated from

$$V_{cv} \sim \xi V_{sw} (r/R_M)^3 \quad , \tag{9.10}$$

where $R_M$ is the magnetopause distance and $\xi$ is the efficiency of the reconnection process in harnessing the solar wind momentum ($\sim 0.1$ for the Earth).

An indication of whether magnetospheric circulation is driven by the solar wind or the planet's rotation can be found by comparing the corresponding electric fields. Since $E_{co} \propto r^{-2}$ and $E_{cv} \propto r^3$ it seems reasonable to expect that corotation would dominate close to the planet while solar wind convection would dominate outside a critical distance $R_c$. Thus the fraction of the magnetosphere that corotates is

$$\frac{R_c}{R_M} = \left( \frac{}{\xi V_{sw}} \right) . \qquad (9.11)$$

This simply says that magnetospheres of rapidly rotating planets with strong magnetic fields will be dominated by rotation while the solar wind will control the plasma flows in smaller magnetospheres of slowly rotating planets.

Now that we have covered the basic ideas underlying generalised magnetospheric theories let us consider the various planets in the solar system and see how well these simple ideas match observations.

## 9.2 PLANETARY MAGNETOSPHERES

In the preceding discussion magnetospheres were characterised using a few key properties of the central object and the plasma flow in which it is embedded. Figure 5 shows values of the corresponding parameters for the nine planets in the solar system. In the top panel there is a logarithmic plot of the size of the planetary system against distance from the sun. The regular spacing illustrates Bode's empirical law.

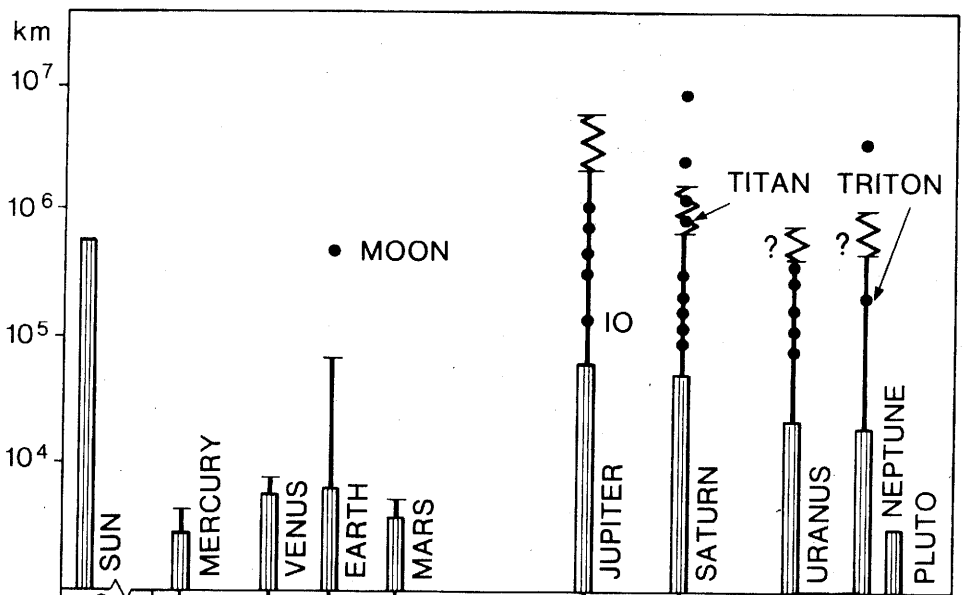


| a (A.U.) | 0.4 | 0.7 | 1.0 | 1.5 | 5.2 | 9.5 | 19.2 | 30 | 39 |
|---|---|---|---|---|---|---|---|---|---|
| $M/M_\oplus$ | $4\times10^{-4}$ | $\langle 2\times10^{-3}$ | 1.0 | $\langle 2\times10^{-4}$ | $4\times10^{5}$ | 560 | ~60? | ~60? | |
| $n_{sw}$ | 26 | 9 | 4 | 2 | 0.2 | 0.05 | 0.01 | 0.005 | |
| $T/T_\oplus$ | 58.6 | -243 | 1 | 1.03 | 0.41 | 0.44 | ~0.65 | ~0.75 | |
| $R_c/R_M$ | $10^{-4}$ | - | 0.2 | - | 2.3 | 1.9 | - | - | |

Figure 9.5 Planetary magnetospheres (after Siscoe, 1979). Each hatched bar corresponds to the planet's radius. The barred line shows the extent (variable for the outer planets) of the planet's magnetosphere. Note the scales are logarithmic. The locations of the major satellites are indicated with dots. An astronomical unit (A.U.) is $1.5\times10^8$ km. The magnetic moment of the Earth, $M_\oplus$ is $8\times10^{25}$ Gauss cm$^3$ ($8\times10^{15}$ Tesla m$^3$). The Earth's rotation period, $T_\oplus$ is 24 hours.

It is traditional to regard the Asteroid belt as dividing the smaller inner planets from the outer giants (Pluto is the awkward exception). This crude division also holds more or less for the size of the planets' magnetospheres. Of the inner planets Earth has by far the strongest magnetic field (moment $M_\oplus = 8\times10^{15}$Tesla $m^3$) with the only other positive measurement being that of Mercury's much weaker field. Upper limits of $2\times10^{-3}M_\oplus$ and $2\times10^{-4}M_\oplus$ have been placed on the intrinsic magnetic fields of Venus and Mars respectively. Thus the plasma environments around these inner planets are strongly influenced by the solar wind and only the Earth has an appreciable magnetosphere.

In the outer solar system a combination of strong planetary magnetic fields and a more tenuous solar wind produces very large magnetospheres. In fact the magnetosphere of Jupiter is the largest 'object' in the solar system, occupying over 300 times the volume of the sun. At present it is not known if Uranus, Neptune or Pluto have intrinsic magnetic fields and their inclusion in the group of giant magnetospheres is speculative (and probably wrong in the case of Pluto). The magnetospheres of Jupiter and Saturn are sufficiently large to envelop most of their natural satellites. These satellites in turn provide most of the magnetospheric plasma.

With the exceptions of Mercury and Venus the rotation periods of the planets do not differ greatly from an Earth day. Nevertheless, when one considers the effect of planetary rotation on magnetospheric circulation relative to the influence of the solar wind, it is clear from the values of $R_C/R_M$ in Figure 5 that rotation dominates throughout the giant magneospheres, for only $\sim$ 20% of the Earth's and to a negligible extent in the rest.

With these generalizations in mind we shall now embark on a tour of the solar system and consider each planetary magnetosphere in turn.

### 9.2.1 Mercury

Mariner 10 was the only spacecraft to visit Mercury, making three flybys between March 1974 and March 1975. Two of these were close to the nightside of the planet where the magnetospheric signatures of a bowshock, magnetopause and magnetotail were detected by the Mariner 10 magnetometer and particle detectors (reviewed by Ness,1979). Nevertheless the magnetic field was found to be weak ($M_{Me} \sim 4\times10^{-4}M_\oplus$) and the magnetosphere small with a stand-off (noon magnetopause) distance $R_M \sim 1.3 \pm 0.2\ R_{Me}$, (Figure 6). Siscoe and Christopher (1975) calculated the variation in the stand-off distance with expected changes in the solar wind ram pressure and predicted that the solar wind would directly impinge on the surface of Mercury a little under 1% of the time. With a negligible atmosphere and no satellites the solar wind is the only source of plasma for the Mercury's magnetosphere. However there are no stably-trapped particles; scaling from the Earth's magnetosphere (discussed in section 9.2.4) would put any plasmasphere well inside the body of the planet. Scaling from the Earth also predictsthat the region on Mercury's dayside where solar wind is funnelled into the magnetosphere (the 'polar cusp') to extend down to 50-60° latitude

nightside, Mercury is expected to have a larger auroral region (extending to 25-35° compared with 70°for the Earth) where material from the magnetotail precipitates on to the surface of the planet. Mercury's weaker magnetic field also means the planet is not shielded from energetic solar particles or cosmic rays.

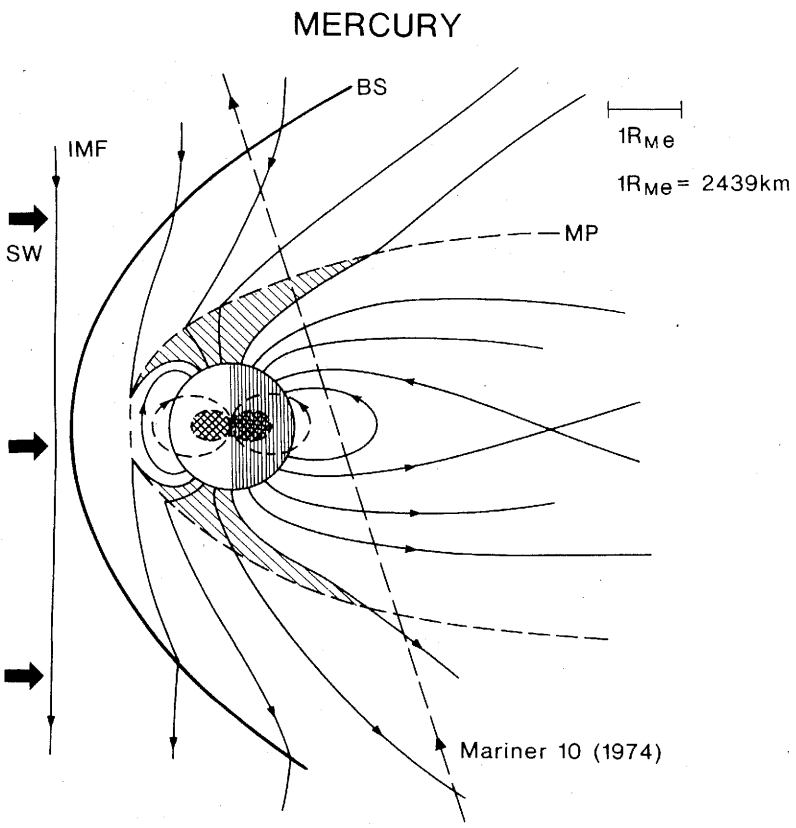


Figure 9.6 The magnetosphere of Mercury. The hatched region outside the planet is the polar cusp. The double hatched region inside Mercury corresponds to the Earth's plasmasphere scaled to Mercury. The trajectory of Mariner 10's third fly-by is the dashed line. The direction of the interplanetary magnetic field is labelled IMF.

Moreover, in Mercury's magnetotail the particle instruments on Mariner 10 detected 4 bursts of energetic particles which lasted for about 1 minute, separated by about 6 minutes. Siscoe et al.(1975) proposed that these bursts are evidence of nightside reconnection events (substorms), the timescale being about 1/20 that at the Earth because of the small spatial scale of Mercury's magnetosphere and the lack of an ionosphere to dampen the motion of magnetic fluxtubes. Thus, although Mercury's magnetosphere is very small and contains no trapped plasma populations its very simplicity could well make it more suitable for investigating nightside magnetic reconnction than the Earth's magnetosphere.

### 9.2.2 Venus

Although early missions to Venus (Venera 4 and 6, Mariner 5 and 10) detected and later extensively mapped (Venera 9 and 10) an upstream bowshock, the Pioneer Venus Orbiter (PVO) was the first spacecraft to explore deep into the Venusian magnetosphere with a full complement of particle and field instrumentation. From the random orientation of the magnetic field measured by the PVO magnetometer behind the planet and the lack of correlation between magnetic signatures and surface features, Russell et al.(1980) concluded that any

dipole moment of Venus is less than $5 \times 10^{-5}$ that of the Earth ($M_V = 0 \pm 5.5 \times 10^{11}$ Tesla $m^3$). Thus the 'magnetosphere' of Venus is the result of the interaction of the solar wind with the planet's atmosphere rather than with an intrinsic magnetic field (reviewed and compared with cometary interactions by Russell et al.,1982).

The fact that the bowshock upstream of Venus is relatively weaker than the terrestrial bowshock suggests that some ($\leq 1\%$) of the solar wind flow is absorbed rather than deflected by the planet. Behind the bowshock the subsonic magnetosheath flow is compressed in front of the planet (Figure 7). This 'squeezing' of the tubes of interplanetary magnetic flux causes the constituent plasma to evacuate along the field and the magnetic pressure to increase. The degree of plasma depletion depends on the relative timescales for plasma evacuation compared with convection of the flux tube. The flow comes close to stagnation ($\leq 20$ km $s^{-1}$) at the sub-solar point which should be compared with a thermal speed of about 100 km $s^{-1}$ for shocked solar wind protons. Thus the dynamic pressure of the solar wind is essentially replaced by the Maxwell stress in the compressed flux tubes. With the upper atmosphere of Venus being strongly ionised by solar ultraviolet radiation a boundary (the ionopause) is formed between the two plasma populations at the altitude where the thermal pressure of the ionosphere balances the magnetic pressure of the compressed solar wind (i.e. at $R_o$ $(nkT)_{ionoshpere} \simeq \frac{1}{2}B^2/\mu_o \simeq (\rho V^2)_{solar\ wind}$). The peak ionospheric

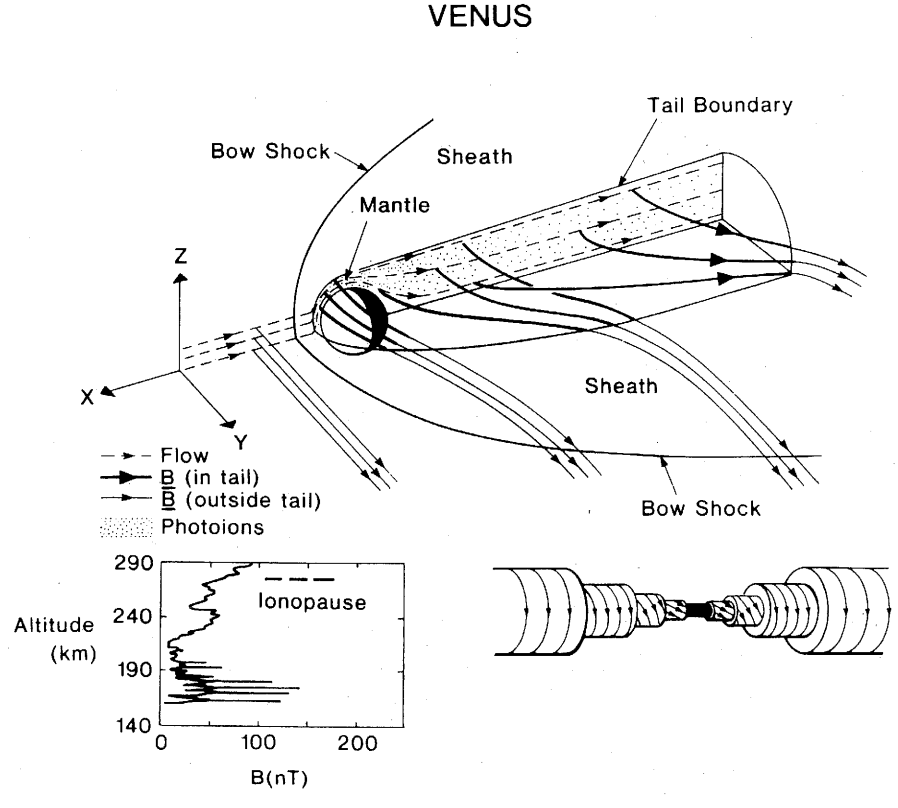


Figure 9.7 (Top) The interaction of the solar wind with Venus (after Saunders and Russell,1985). (Bottom left) An example of the magnetic field measured by PVO inside Venus' ionosphere (Phillips et al.,1984).

ionopause height of 250-300 km. Therefore, with exception of rare occasions when the solar wind dynamic pressure exceeds the peak ionospheric pressure ($\leq$ 15% of the time), one would expect the IMF to be excluded from Venus by its conducting ionosphere and the solar wind to be deflected around the planet.

Although PVO indeed measured average magnetic fields close to zero in the ionosphere, the spacecraft frequently encountered small regions of high magnetic fields even under quiet solar wind conditions. The magnetic field in these regions tended to be twisted up into 'fluxropes' as illustrated in Figure 7 (Russell and Elphic,1979). The origins of these flux ropes are unknown though it seems plausible that small bundles of magnetic flux are either "sheared-away" (by the Kelvin-Helmholtz instability) at the ionopause or just dragged through the ionosphere by the magnetic tension along the field lines exerted ultimately by the solar wind.

The neutral atmosphere of Venus extends beyond the ionopause into the magnetosheath. Photoionisation (and/or charge exchange with the solar wind protons in the sheath) produces $H^+$, $H_2^+$, $H_e^+$ and $O^+$ ions which are 'picked-up' in the sheath flow and carried downstream past the planet. Moreover, the PVO plasma data showed evidence of blobs of ionospheric plasma being 'scavenged' in some manner and carried away by the sheath flow. The momentum gained by these new or scavenged ions must come from the background plasma flow which is correspondingly decelerated. Thus the interplanetary field lines are 'caught up' and draped over the planet forming a wake or tail downstream. Similar to the Earth's magnetotail, the smaller magnetotail of Venus has two lobes separated by a current sheet. The orientation of the Venus current sheet, however, is determined solely by the direction of the IMF rather than a planetary field (Saunders and Russell, 1985).

Thus the Venus magnetosphere is confined to a relatively small ($\leq$ 0.3 $R_V$) boundary layer where the solar wind interacts with the Venusian ionosphere. In the process, plasma is added to the deflected solar wind flow and the resulting mass-loaded flux tubes are then draped over the planet to form a thin tail ($\sim$ 4 $R_V$ across) downstream.

### 9.2.3 Earth

The Earth's magnetosphere has been explored by many spacecraft over the past two decades. Although the general morphology is well-understood, the present task is to investigate details of the physical processes occurring in different regions (see Chapter 2). In the hierarchy of planetary magnetospheres the Earth comes between the small, solar-wind dominated magnetospheres of the inner planets and the large, rotation-dominated magnetospheres of the giant planets.

Balancing the Earth's dipolar magnetic field pressure with the ram pressure of the solar wind puts the Chapman-Ferraro standoff distance $R_{cf}$ at 8.8 to 10.4 $R_E$. The fact that the average noon position of the Earth's magnetopause is 10.8 $R_E$ suggests that a finite pressure of magnetospheric particles should also be included in the pressure balance. These particles have two sources: plasma escaping from the

Earth's ionosphere populates the inner region of the magnetosphere (plasmasphere) while the solar wind leaks in across the magnetopause on reconnected field lines (see Chapter 5) and populates the outer region of the dayside magnetosphere and the magnetotail(Figure 8). The energetic particle population in the Van Allen radiation belts consists of protons and helium ions (presumably from the solar wind) mixed with oxygen ions from the ionosphere. The relative proportion of radiation belt particles with solar wind or ionospheric origins is not known and probably varies with solar wind conditions.

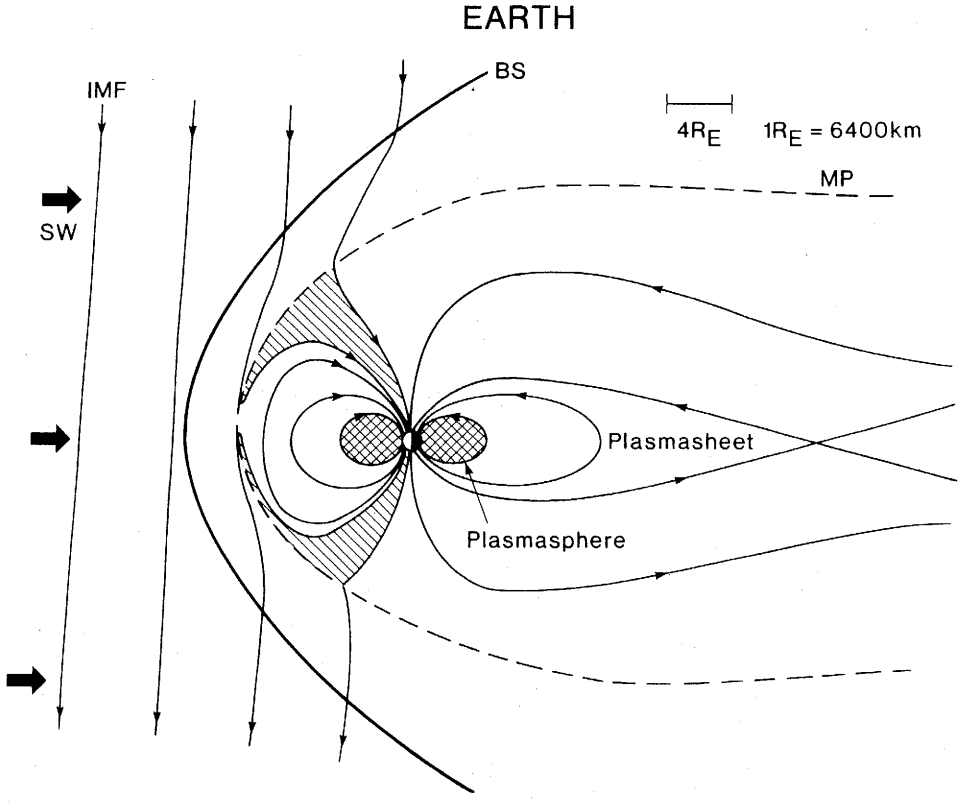


Figure 9.8 The Magnetosphere of the Earth.

The low energy plasma inside the plasmasphere largely corotates with the Earth. The plasmapause is the boundary (at $\sim 4R_E$) where the magnitude of electric field associated with reconnection exceeds the corotational electric field. Thus outside the plasmasphere the plasma circulation is driven by the solar wind (Chapter 5).

The Moon, $66R_E$ from the Earth, spends less than 10% of its orbit inside the Earth's magnetosphere. The early spacecraft Explorers 33 and 35 carried magnetometers and plasma detectors to investigate the interaction of the solar wind with the Moon. First they discovered there was no bow shock upstream of the Moon. When the spacecraft later passed behind the Moon, downstream of the object, the perturbations in magnetic field (Figure 9), the plasma density rarefaction and deflection of the solar wind flow,were found to be consistent with supersonic flow around a non-conducting body (Taylor et al.,1968). Models of the solar wind interaction with a non-conducting body (Figure 1a) such as the Moon have been developed by Spreiter et al.(1970).

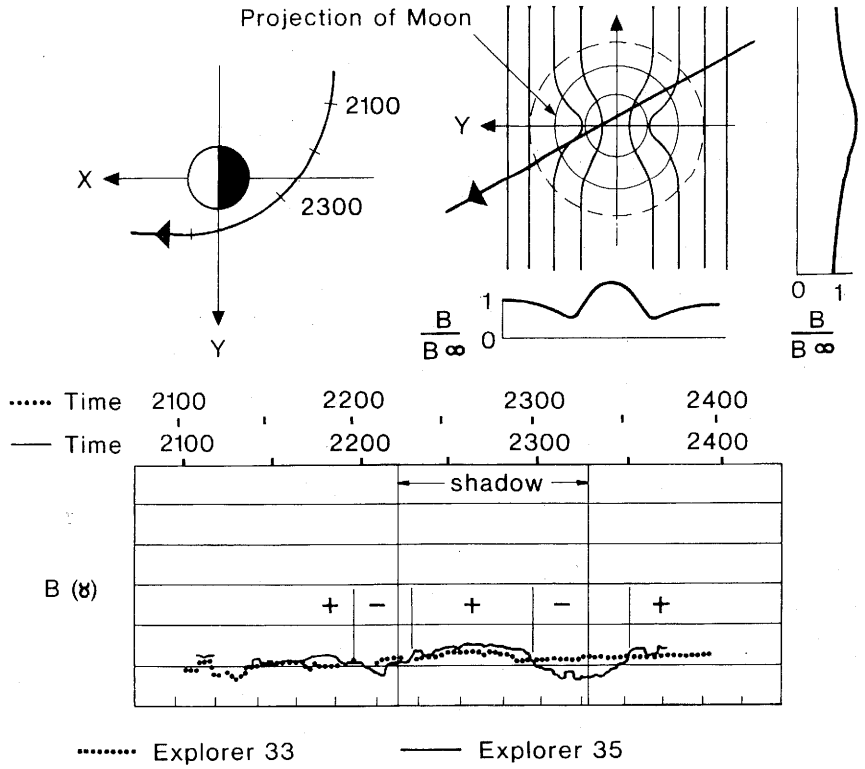


Figure 9.9 The interaction of the solar wind with the Moon. Top right shows the magnetic field perturbations that would be expected if the Moon is a non-conductor. The arrowed line is the spacecraft trajectory. (Below) The magnetic field signatures observed by Explorers 33 and 35 in 1967 (from Spreiter et al.,1970).

### 9.2.4 Mars

Although Mariner 4 indicated the presence of a bow shock as early as 1965, there has been very limited exploration of the solar wind interaction with Mars. Soviet spacecraft Mars 2,3 and 5 carried magnetometers and confirmed the presence of a bow shock (at $1.5\pm0.15$ $R_{Ma}$). Unfortunately, none of these spacecraft reached altitudes less than 1000km and the interpretation of the scant data sets has become a controversial subject. While some put forward evidence of a small intrinsic magnetic field (Dolginov,1978; Slavin and Holzer,1982) others claim there is no need to invoke entry into a Martian magnetosphere to explain the data (Russell,1978; Russell et al.,1984). The most optimistic upper limit on the planetary field ($2 \times 10^{-3}$ $M_\oplus$) was given by Dolvinov (1978) by assigning a wake boundary as a magnetopause. On the other hand Russell(1978) suggested that the wake boundary is due purely to draping of the IMF and brought the limit down to ($2.5 \times 10^{-5} M_\oplus$). More recently, Slavin and Holzer (1982) have suggested an intermediate value of $1.8\pm0.8\times10^{-4}$.

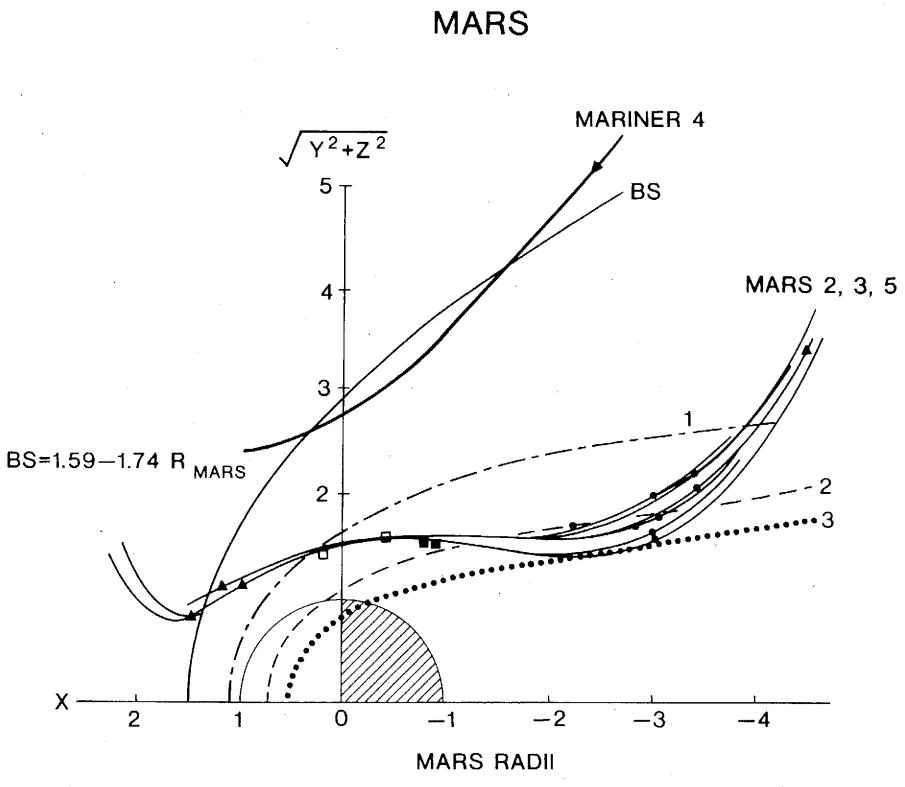


Figure 9.10 The interaction of the solar wind with Mars. The locations of Mars 5 'magnetospause' crossings, as identified from magnetometer data, are shown by squares and dots. The triangles are bowshock crossings. Line 1 is the maganetopause location scaled from the Earth to be consistent with the observed bowshock location. Line 2 is the best fit to the magnetopause crossings using a scaled terrestial magnetopause. Line 3 is the largest scaled terrestial maganetopause consistent with the observations under the assumption that none of the magnetopause encounters are in fact encounters with the planetary magnetic field. (After Russell, 1978).

In any case, the interaction with the solar wind will be confined to a small region very close to planet. The atmosphere of Mars is much less dense than that of Venus and therefore it is unlikely that the pressure of ionospheric material could stand off the solar wind. Thus it is expected that the majority of the solar wind slips around a conducting outer layer with limited entrainment of ionospheric plasma and the IMF is weakly draped over the planet in a small downstream wake.

### 9.2.5 Jupiter

When Burke and Franklin (1955) discovered, somewhat by accident, that Jupiter is a source of radio emission, it was soon realised that this radio emission must come from energetic charged particles in a strong magnetic field. This remarkable discovery came before Van Allen's detection of the Earth's radiation belts and the in situ verification of the solar wind (Neugerbauer and Snyder, 1962). A more puzzling discovery came a few years later when Bigg (1964) revealed that the low frequency (decametric) component of the Jovian radio emission was

magnetic field; the high frequency cutoff indicated the great strength of the Jovian magnetic field ($M_J \simeq 4 \times 10^5 M_\oplus$). Moreover, from the periodic variations in the high frequency (decimentric) component of the radio emission it was possible to determine Jupiter's rotation period accurately and the 9.6° tilt of the magnetic dipole with respect to the planet's rotation axis. The low frequency emission was assumed to be synchrotron radiation from electrons with energies of $\sim$ 10 MeV that gyrate around dipolar magnetic field lines at a radial distance of a few times the radius of Jupiter (1 $R_J$ = 71400 km). This basic picture of a strong magnetic field trapping a large, energetic particle population was confirmed by the Pioneer 10 and 11 spacecraft which reached Jupiter in December 1973 and 1974 respectively. The Pioneers also revealed that farther from the planet the magnetic field is considerably stretched out so that the Jovian magnetosphere is shaped more like a disc than a sphere (Figure 11). Although the large size ($R_M$ = 50-100 $R_J$) and radial distension implied the presence of a substantial amount of plasma at lower energies, the Pioneer plasma detector provided little information of the thermal population. Nevertheless, the theorists had already come out strongly in favour of a magnetosphere dominated by the planet's rotation (Gledhill,1967; Melrose,1967; Brice and Ioannidis,1970).

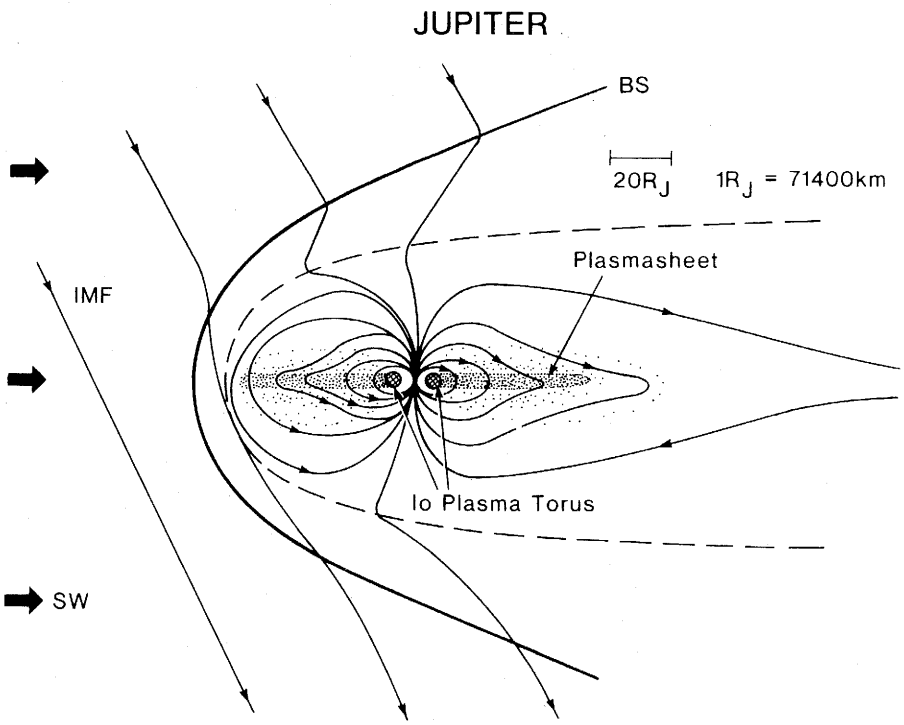


Figure 9,11 The magnetosphere of Jupiter.

A few months before the Pioneer 10 encounter, Brown (1974) detected optical (d-line) emission from a cloud of neutral sodium atoms in the vicinity of Io using a ground-based telescope. The first direct evidence of the presence of ionised material at low energies near Jupiter came with the discovery by Kupo et al. (1976) of optical emission $S^+$ ions. Brown (1976), borrowing techniques from studies of more remote astronomical gaseous nebulae, concluded that the $S^+$ emission came from a dense ring of cold plasma inside the orbit of Io. The Voyager 1 and 2 spacecraft confirmed that Io is the major source of plasma in the Jovian magnetosphere, a fact that seemed less surprising when the Voyager cameras revealed the satellite's active volcanos.

(i) The Io-plasma interaction

Bigg's observation that Io modulates the intensity of the Jovian decametric radio emission initiated many early models of the satellite's interaction with the magnetospheric plasma (Marshall and Libby,1967; Piddington and Drake,1968; Goldreich and Lynden-Bell,1969; Gurnett,1972; Geortz and Deift,1973). These early studies assumed Io was a perfect conductor and the ambient plasma density very low. They examined how Io's motion in the planetary magnetic field might cause the satellite to act as a unipolar generator and investigated the possibility that large field-aligned currents might directly connect the satellite to the planet. Following Drell's description of a large conducting body generating Alfven waves as it moves through a magnetic field (Drell et al.,1965), Marshall and Libby (1967) were the first to propose that Io might generate large amplitude Alfven waves that propagate along the magnetic field to the ionosphere ofJupiter where the radio bursts are triggered. However, in applying the theory to Io, the early theorists were hampered by the fact that very little was known about the properties of Io and the surrounding plasma.

The large perturbations of the magnetic field that were measured in the vicinity of Io when Voyager 1 passed beneath the satellite confirmed the theoretical expectations of a strong interaction between Io and the magnetospheric plasma. Indeed, further analysis of the Voyager 1 observations indicated that an Alfvenic disturbance was radiated by Io, carrying a $\sim 10^6$ amp field-aligned current towards the ionosphere of Jupiter (Belcher et al.,1981). Moreover, the observed high plasma densities implied that the propagation speed of Alfven waves is small in the torus. This means that by the time an Alfven wave has travelled from Io to the ionosphere (where it is reflected) and back, Io has moved along its orbit so that the field-aligned currents do not form a closed loop as first suggested by Goldreich and Lynden-Bell(1969) but rather form open-ended Alfven wings similar to Drell's model. Neubauer(1980), Geortz(1980) and Southwood et al.(1980) have developed theoretical models of Io's interaction with the magnetospheric plasma which incorporate some of the basic Voyager results and involve the generation of large amplitude Alfven waves.

Although it seems that to first approximation Io is a good conductor, in detail the Io-plasma interaction is complicated; for example, one should consider the presence of a neutral atmosphere, local ionisation of neutral material by the corotating plasma and the sputtering of energetic charged-particles on the satellite's surface which in turn generates more plasma.

Concerning the Io-modulation of the decametric radio emission, there have been attempts to relate features of the emission to models of the Io-generated Alfven waves (Gurnett and Goertz,1981; Bagenal,1983) but it has not yet been proved that there is a causal relationship between the two phenomena.

(ii) The Io plasma torus

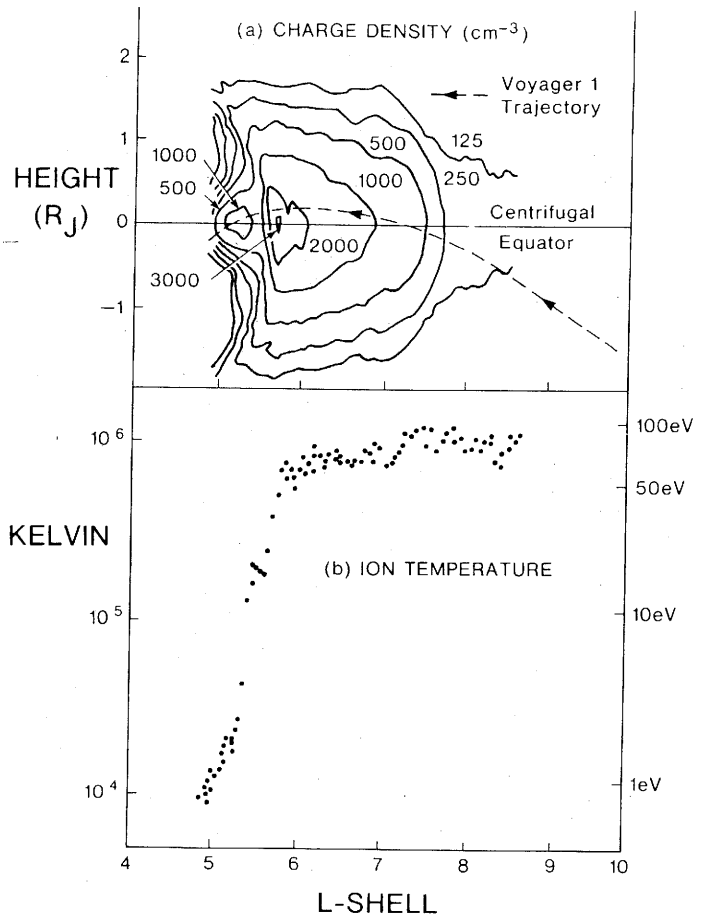


Figure 9.12 Voyager 1 measurements of positive ions in the Io plasma torus. (a) Contours of positive charge density (equal to the electron density). (b) Ion temperature.

toroidal region encompassing the orbit of Io. The observed spectrum indicated the emission was coming from ions of sulphur ($S^+$, $S^{2+}$, $S^{3+}$) and oxygen ($O^+$, $O^{2+}$). When the Voyager spacecraft later flew through the plasma torus, the Plasma Science instrument made in situ measurements of both the electrons and the various positive ionic species. From the Voyager plama measurements (Figure 12) it is clear that the Io plasma torus is divided into two distinct regions with a sharp boundary at 5.7 $R_J$, inside Io's orbit (5.9$R_J$)(Bagenal and Sullivan,1981;but see Bagenal et al.,1985). It is the large outer region of warmer (∿80eV) plasma that produces the UV emission while the optical emissions come mainly from the much colder (∿1eV) plasma inside 5.7 $R_J$.(The spectrophotometry of the Io plasma torus is reviewed by Brown et al.,1983). It is estimated that at least $10^{28}$ ions must be produced by Io per second to maintain the plasma torus but the actual source mechanism is not known. Two possibilities are that (i) plasma is produced directly in the interaction between the satellite and the magnetospheric plasma; or (ii) neutral material is sputtered off the satellite's surface and escapes to form a large neutral cloud that is later ionised. The tenuous atmosphere of Io and the lack of enhancd UV emission near Io limit the source strength from the first mechanism and recent detection of emission from extended neutral clouds of oxygen (Brown, 1981) and sulphur (Durrance et al., 1983) favour the second mechanism.

In either case, when the neutrals are ionised they experience a Lorentz force due to their motion relative to the local magnetic field; this force causes the ions to gyrate about the magnetic field at a speed equal to the magnitude of the neutral's initial velocity relative to the surrounding plasma (Figure 13). The ion is accelerated until its guiding centre motion matches the plasma rest frame, corotating with Jupiter. Because a particle's gyro-radius ($R_g$) is mass-dependent, the new ion and its electron are separated after ionisation. Hence there is a radial current due to the ions being 'picked-up' by the magnetic field. This radial current across the torus is linked by field-aligned (Birkeland) currents to the ionosphere of Jupiter where the $\underline{J}x\underline{B}$ force is in the opposite direction to the planet's rotation. Thus the planet's essentially-limitless source of angular momentum is tapped electrodynamically by the newly ionised plasma.

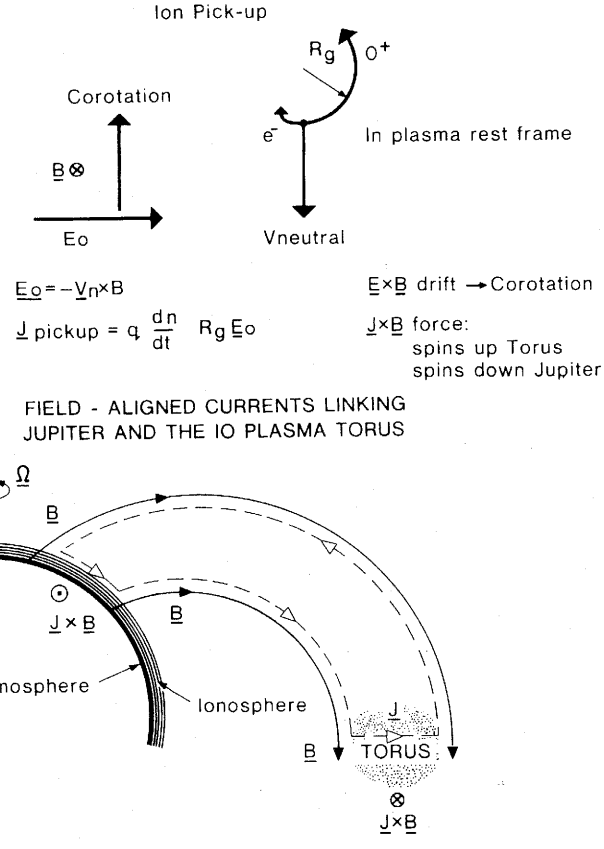


Figure 9.13 Ion pick-up ion the Io plasma torus.

Oxygen and sulphur ions 'picked up' by the magnetic field gain gyro-energies 170 and 540 eV respectively. The initial velocity distributions are highly anisotropic and the different ionic species and electrons are not in thermodynamic equilibrium. Coulomb collisions between ions or with electrons will change the distribution to a more stable one (Maxwellian). The effects of collisions over increasing timescales are: firstly to make the velocity distribution of each ionic species isotropic; secondly, to produce equipartition of energy for each species; and thirdly, to produce equipartition of energy between ions of different mass (including eventually the electrons).

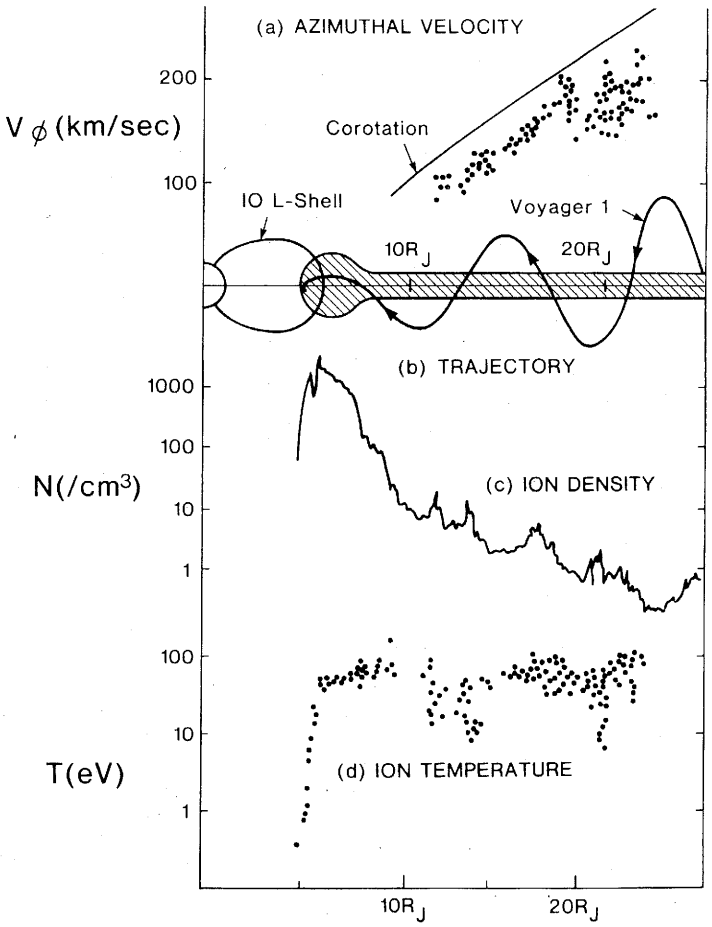


Figure 9.14 Voyager 1 ion measurements in the Jovian plasmasheet. (a) Azimuthal velocity; (b) the spacecraft trajectory in magnetic co-ordinates; (c) ion density; (d) ion temperature.(After Belcher,1983).

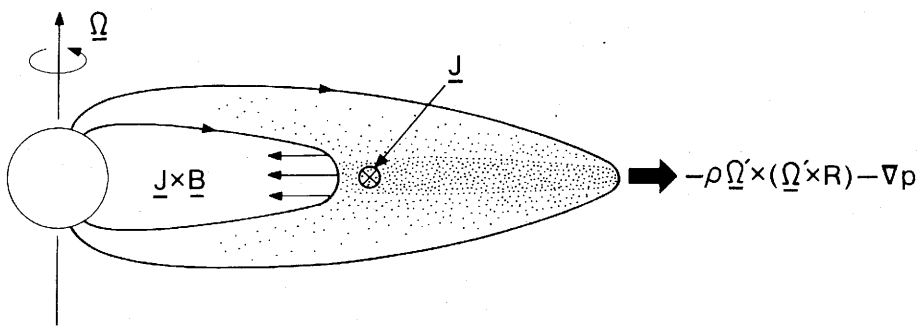


Figure 9.15 Local radial force balance in the plasma sheet (after McNutt,1983).

(v) Magnetotail

There is a limit to the distance at which a fluxtube of given plasma content can be maintained at corotation by an inward magnetic stress. This distance is thought to be where the corotation speed is of the order of the local Alfven speed. On the dayside of the magnetosphere the solar wind may provide sufficient inward stress to keep the fluxtube inside the magnetosphere. On the nightside the fluxtube would be free to move outward down the tail in a planetary wind (Hill, Dessler & Michel,1974). Vasyliunas(1983) suggests that the planetary wind will extend the magnetic field lines until they reconnect, breaking off plasmoids which then travel down the magnetotail (Figure 16).

Although the basic ideas of diffusive transport in the inner magnetosphere have been confirmed we are a long way from a full description. It is clear that slow inward diffusion allows time for the plasma to radiatively cool but it is not possible to match both the low temperatures and the observed ionic composition in the inner torus with the simple model described above; the data suggest there must be an additional source of plasma and a considerable energy sink well inside Io's L-shell (Richardson and Siscoe,1983; Bagenal,1985). Radially outward from Io, where diffusion is quite rapid, there is insufficient time for the plasma to either cool by radiation or come to thermodynamic equilibrium as it diffuses outwards. With comparable timescales (tens of days) for plasma transport, production, energy losses and thermal equilibrium it is a formidable task to derive a full description of the multi-component plasma as a function of radial distance in the warm torus. Furthermore, the erratic nature of Io's volcanos, the ultimate source of the torus material, would suggest a non-steady state. Indeed, the emissions from the torus plasma show a considerable degree of temporal variability (Brown et al.,1983).

Still farther out in the Jovian magnetosphere, the simple picture of radial transport by fluxtube interchange is complicated by a substantial pressure of energetic particles and a significant departure of the magnetic field from that of a dipole.

(iv) Plasmasheet

As the plasma diffuses outwards from the Io plasma torus it remains confined to the centrifugal equator forming a thin, disc-shaped, plasmasheet, tilted by $\sim 7°$ from the rotation equator. Thus, when Voyager traversed the magnetosphere, the plasma detector measured enhanced densities and lower temperatures (Figure 14c & d) every time the disc rotated past the spacecraft. Although the bulk motion of the plasma remained azimuthal, the velocity ($\underline{V}_\phi = \underline{\Omega}' \times \underline{r}$) lagged behind strict rotation ($\underline{\Omega} \times \underline{r}$), indicating that the conductivity of the ionosphere is insufficient to carry the currents required to enforce rigid corotation (Figure 14a). At the same time, the magnetic field lines are stretched out by the mechanical stresses on the plasma. Alternatively, one can think of the mechanical stresses on the plasma giving rise to charge-dependent drifts which constitute an azimuthal or "ring" current. For a thin plasmasheet the steady-state magnetic field configuration and plasma distribution are given by considering the balance of stresses. Locally the force density, viewed either as arising from the Maxwell stresses of the stretched-out field lines or equivalently as the $\underline{J} \times \underline{B}$ force of the magnetic field acting on the current sheet, must balance the mechanical stresses on the plasma (Figure 15) (McNutt, 1983). Globally, the large-scale pattern of the currents and the source of the mechanical stresses need to be considered. The present task of finding a self-consistent quantitative model, compatible with the Voyager and Pioneer observations, is reviewed by Vasyliunas(1983b).

the timescale for transport (i.e. days).

The distribution of plasma along magnetic field lines is limited by the strong centrifugal forces which tend to confine the plasma to the region of the field line farthest from the rotation axis, the centrifugal equator. To first approximation the plasma density, n , decreases exponentially with distance from the centrifugal equator

$$n(z) = n(0)\ \exp-(z/H)^2, \qquad (9.12)$$

where the scale height H is given by $H=(2kT_i/3m_i\Omega^2)^{\frac{1}{2}}$ for ions of mass $m_i$ and temperature $T_i$. Thus the warmer ions in the outer region of the torus have a larger scale height and are more spread out along the field than the cold ions inside Io's orbit (see Figure 12).

(iii) Radial transport

In the region dominated by rotation in the Earth's magnetosphere plasma is re-distributed by episodic escape of material through the dayside magnetopause followed by thermal diffusion of plasma from the ionosphere along magnetic field lines, re-filling the plasmasphere within several hours. The strong magnetic field of Jupiter means that the inner Jovian magnetosphere is more rigid (i.e. sheltered from gusts in the solar wind). Moreover, the main plasma source is restricted to the L-shell of Io ($L\approx5.9$). Therefore the re-distribution of material in the inner magnetosphere must occur on much longer timescales by diffusion <u>across</u> L-shells. The diffusive process is thought to be via a random, small scale interchange (or 'mixing') of fluxtubes. Gold(1959) pointed out that in a low-$\beta$ plasma whole fluxtubes can be interchanged without a change in magnetic energy. If the energy of the plasma in two fluxtubes differs, the interchange motion may release or absorb energy. In the former case the system is unstable (Sonnerup and Laird,1963). At Jupiter fluxtube interchange is under the influence of the centrifugal force which aids outward but inhibits inward transport (Siscoe and Summers,1981). Therefore plasma preferentially diffuses radially outwards from Io's L-shell while the inward diffusion is very slow.

Since fluxtube interchange conserves magnetic flux the diffusing quantity is the plasma density per unit magnetic flux which, for a dipole field, is directly proportional to $NL^2$ where N is the density per unit L-shell. The steady state diffusion equation is then

$$L^2\ \frac{d}{dL}\left[\frac{D}{L^2}\ \frac{d}{dL}(NL^2)\right] + \text{Sources} + \text{Losses} = 0\ , \qquad (9.13)$$

where D is the diffusion coefficient(Dungey,1965; Siscoe,1979). The radial profile of $NL^2$ derived from the Voyager plasma data (Bagenal and Sullivan,1981) has a maximum at 5.7 $R_J$ which supports the idea of diffusion of plasma from a single source near Io. The asymmetry of the transport process, imposed by the centrifugal potential, is evident in the slope of the $NL^2$ profile. The steeper slope inside $5.7R_J$ implies a larger diffusion coefficient (Richardson and Siscoe,1981).

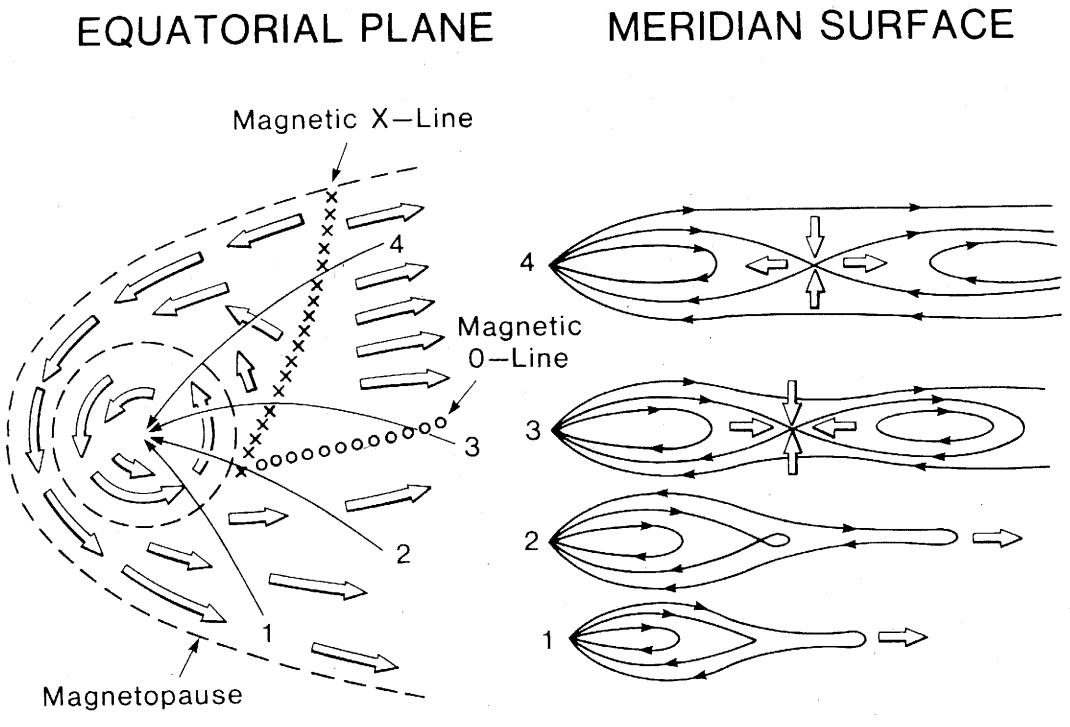


Figure 9.16 A sketch of plasma flow (large arrows) in the equatorial plane (left) and a sequence of meridian surfaces (right) expected from the planetary wind model (from Vasyliunas,1983b).

In conclusion, it is clear that the magnetosphere of Jupiter is radically different from the magnetosphere of the Earth; a large fraction of the Jovian plasma population comes from the satellite Io and rotation dominates the plasma dynamics. Recent reviews of various aspects of the physics of the Jovian magneosphere can be found in Dessler(1983).

### 9.2.6 Saturn

In the two years between September 1979 and August 1981 the magnetosphere of Saturn was explored by three spacecraft, Poineer 11 and Voyagers 1 & 2. Pioneer 11 detected a planetary field ($M \simeq 560\ M_0$) with a symmetry axis very closely aligned (within 1°) to the planet's rotation axis. Overall, the magnetosphere of Saturn was found to be similar to the Jovian magnetosphere: satellites are the major source of magnetospheric plasma and the plasma dynamics are dominated by the planet's rotation. Nevertheless the magnetosphere of Saturn is considerably smaller and the plasma sources much weaker than at Jupiter. Moreover, the dayside magnetopause at Saturn was found close to the Chapman-Ferraro distance (equation 9.2) at 20 $R_S$ which indicates that it is the planetary field which stands off the solar wind, with a little contribution from the internal plasma pressure (Figure17).

(i) Sources of plasma

The detection of substantial densities of oxygen ions as well as protons

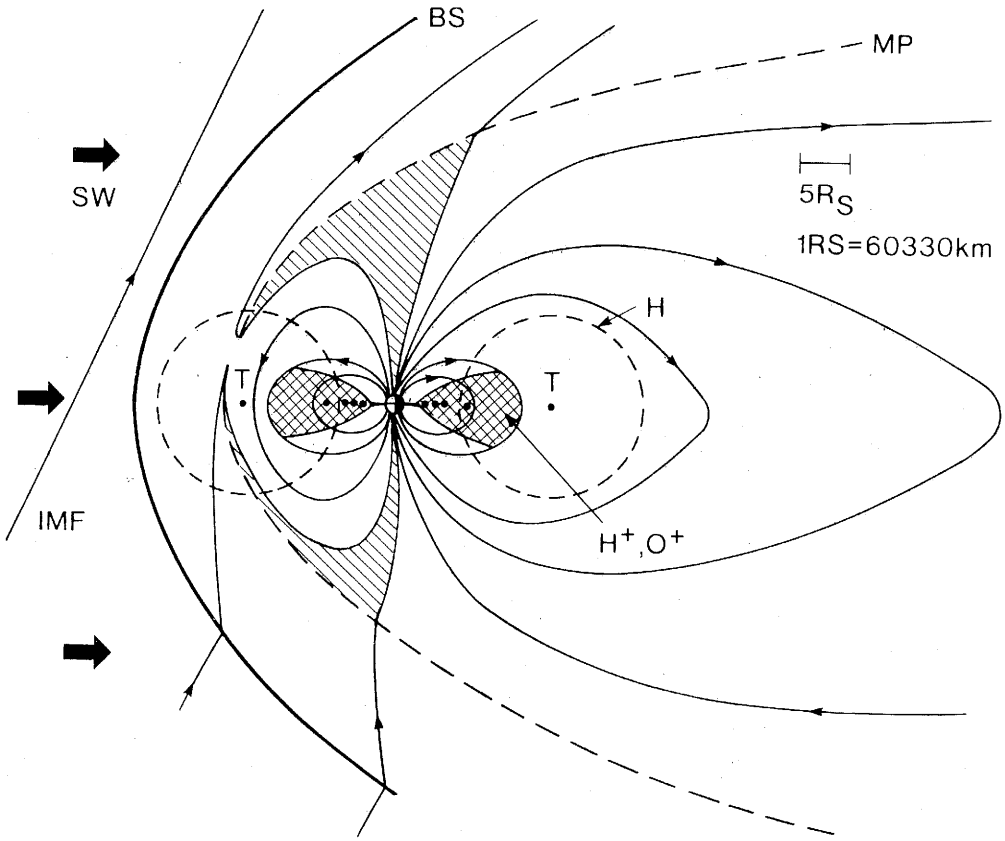


Figure 9.17 The magnetosphere of Saturn. The single hatching shows the polar cusp. The double hatching shows the toroidal region of satellite ions. The dashed circle indicates the cross-section of the neutral hydrogen torus around the orbit of Titan (T).

in the region of the orbits of Saturn's icy satellites (Rhea, Dione and Tethys at 8.8, 6.3 and 4.9 $R_S$ respectively) indicates that the satellites must be major sources of plasma. Recent studies of the Voyager plasma data (Richardson,1985) have revealed the amount ($NL^2$) of $O^+$ ions has a maximum at L≈10 which suggests tha ion production is not a direct result of plasma interaction with the satellites but probably involves a cloud of neutral atoms that extends beyond the satellite orbits. These fairly small (radii ⩽ 800 km) icy satellites have negligible atmospheres and are probably poor electrical conductors so that the corotating plasma and energetic particles impinge on the surface, sputtering off the neutral atoms. In contrast, in the outer magnetosphere, the much larger satellite Titan (radius ≈ 2575 km) has a substantial nitrogen atmosphere and is a direct source of heavy ions $N^+$ and possibly $N_2^+$ or $H_2CN^+$ (Hartle et al.,1982). The Voyager ultraviolet spectrometer detected strong emission from a large toroidal cloud of neutral hydrogen between 8 and 25 $R_S$ (Broadfoot et al.,1981). This neutral H cloud must be a source of magnetospheric protons in addition to some, as yet undetermined, combination of icy satellite, solar wind, and ionospheric sources.

(ii) Interaction of magnetospheric plasma with Titan

The passage of Voyager 1 close to Titan provided a unique opportunity to study the interaction between a plasma flow and a body with an atmosphere. Since the incident magnetospheric plasma flow was transalfvenic ($M_A \approx 1.9$) and subsonic ($M_s \approx 0.57$) no upstream bowshock was observed and the plasma flowed quite smoothly round the satellite. However it is clear that the upper atmosphere of Titan is not sufficiently ionised (or, more specifically, the electrical conductivity is not sufficient) to allow the plasma just to slip around the satellite. The impinging plasma interacts with the uppermost atmosphere, picking up $N^+$, $H^+$, $N_2^+$,etc; from Titan's exosphere. The mass loading of the magnetospheric fluxtubes slows them down and causes them to drape over Titan and form a wake downstream. The wake then resembles an induced magnetotail with the northern and southern lobes containing oppositely-directed field lines. The mass loading appeared to be more effective on the sunlit side of Titan, resulting in an asymmetric wake (Figure 18).

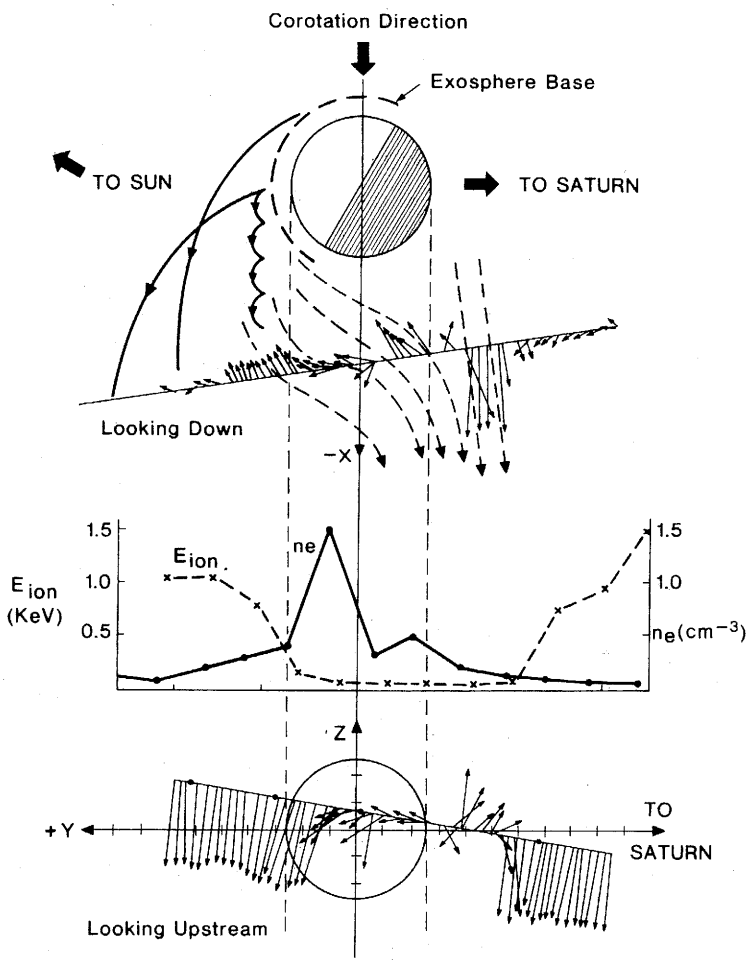


Figure 9.18 The interaction of the magnetospheric plasma with Titan.(Top) The Voyager trajectory with the observed X-Y components of magnetic field (arrows) and inferred plasma flow (dashed lines). The cycloidal motions of hot(cold) ions with large (small) gyro-radii are shown on the sunward side of Titan. (Middle) A plot of the average ion energy ($E_{ion}$) and electron density ($n_e$) measured by Voyager as it passed through Titan's wake. (Bottom) The perturbations of the magnetic field (Y-Z components) show how the planetary field is draped over the satellite. After Neubauer et al.(1984) and Bridge et al.(1981).

(iii) Morphology

Inside L≈15 the plasma is concentrated near the equator forming on extensive plamsa disc. With the plasma temperature decreasing radially

L≈3 where the plasma temperature is less than 1 eV (Lazarus and McNutt, 1983; Sittler et al,1983). This picture of a tapered plasma sheet is consistent with the idea of the plasma cooling as it diffuses in from a source in the outer part of the sheet, and as the plasma cools it must collapse towards the equator. Indeed, the equatorial plasma density was observed to increase from less than 1 $cm^{-3}$ at L≈10 to over 100 $cm^{-3}$ at L≈3. In this inner region the plasma flow is largely azimuthal with a lag behind strict corotation, presumably due to mass loading, in the source region. Between 8 and 16 $R_S$ the plasma has a substantial component at higher energies (10's of keV). The ions and electrons at these energies have a differential azimuthal drift motion producing a $10^7$ Amp ring current which distorts the magnetic field from a dipole by effectively stretching out the field lines in the equatorial region. Thus at Saturn it is the pressure gradient of the hot component rather than the mechanical stresses on the cold plasma (as for example in the Jovian magnetosphere) that balences the JxB force under steady-state conditions (see equation 9.8) (McNutt,1983).

Outside 15 $R_S$ the plasma properties (density, temperature and bulk motion) are highly variable. Embedded in a background of tenuous, hot plasma there appear to be dense, cold blobs or streams. In this outer region the flow is rather erratic with considerable radial and vertical flows (Richardson,1985). The cause of the variability of the plasma in this outer region is not known in any detail but it is clear that the solar wind could be affecting a thick boundary layer in the dayside magnetosphere. On the nightside the solar wind drags the magnetic field out into an extensive magnetotail, similar to the Jovian magnetotail.

In summary, it appears that the magnetosphere of Saturn is similar to the Jovian magnetosphere in that it is large, the plasma motions are dominated by the planet's rotation and satellites are the main source of plasma. However the fact that saturn's satellites are much weaker plasma sources than Io (by about $10^{-2}$) and are distributed throughout the magnetosphere makes a quantitative description less straightforward than at Jupiter. Reviews of various aspects of Saturn's magnetosphere can be found in Gehrels and Mathews(1984).

Finally, it is interesting to note that,although the total energy contents of the magnetospheres of Earth, Jupiter and Saturn vary by orders of magnitude, the ratio of the energy in the trapped particle population to the energy in the magnetic field is approximately the same for the three magnetospheres. It appears that the energy in the plasma builds up to only 1/1000 of the magnetic field energy at which point some sort of plasma instability is presumably triggered, preventing further build up (Schardt,1984).

### 9.2.7 Uranus

Until Voyager 2 flies past Uranus in January 1986 any discussion of a Uranian magnetosphere is largely speculative. The only indication to date that Uranus has a magnetic field comes from recent International Ultraviolet Explorer observations of Lyman-α emission (Clarke,1982; Durrance and Moos,1982). It is not possible to account for the emission

by resonant scattering of solar Lyman-$\alpha$ emission, which makes charged-particle excitation the most likely cause of the emission. The flux of solar wind particles over the disc of Uranus only provides a few percent of the energy of the emission. The observers raised the appealing explanation that the solar wind particles from a much larger area are focussed by a planetary magnetic field. If the emission is confined to an auroral region between 80° and 90° latitude then the observations imply an average surface intensity similar to the measured surface intensities of the Saturnian and Jovian aurorae. Assuming that the energy of the precipitating particles is converted to auroral emission at an efficiency of 5% then the observed auroral intensities require a total precipitated power of about $3 \times 10^{11}$ watts. To provide this power to Uranus' ionosphere the planet's magnetic field would effectively have to funnel the solar wind impinging on a disc of radius 25 $R_U$, which implies a very large magnetosphere. Thus the range of observed emission intensities suggest the magnetic field at the surface of Uranus is between 1 and 10 Gauss. The value predicted by the rather dubious empirical relationship, magnetic Bode's law is 1.7 Gauss (Hill and Michel,1975).

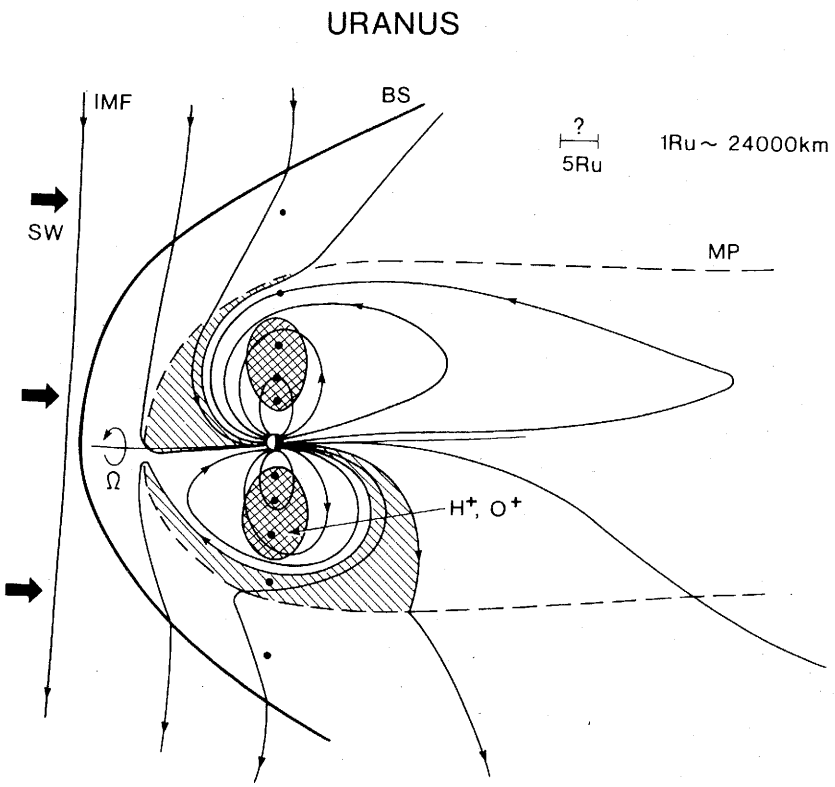


Figure 9.19 The magnetosphere of Uranus. The hatched region shows the position of the polar cusps. The double hatching indicates the expected region of any satellite ions. The cylindrical symmetry of the magnetotail is disturbed by reconnection of the planetary magnetic field with the IMF.

Taking the emissions to imply the existence of a magnetosphere we next consider the possible characteristics of the Uranian magnetosphere. Unlike the other planets, Uranus' axis of rotation lies close to the

towards the sun (Figure 19). Siscoe(1971,1975) pointed out that such a 'pole-on' configuration would produce a magnetosphere with several novel features. Firstly, the sunward-pointing pole would form a cusp funnelling solar wind onto the dayside ionosphere. Secondly, the alignment of the dipole axis with the solar wind would produce an unusual magnetic field topology in the magnetotail. Instead of the usual situation with two adjacent lobes of oppositely-directed magnetic field separated by a planar current sheet, with the 'pole-on' configuration at Uranus the two lobes would form concentric cylinders separated by a solenoidal current sheet. Thirdly, with a polar cusp near the sub-solar point, there is always a region on the magnetopause where the planetary magnetic field is anti-parellel to the IMF. Thus, unlike the Earth's magnetosphere where the occurrence of magnetic reconnection at the magnetopause depends strongly on the direction of the IMF, reconnection could occur at Uranus' magnetopause for all IMF orientations.

In spite of the planet's smaller radius (26,000 km) and slower rotation rate the planet's rotation probably controls the internal plasma flows (i.e. $R_c/R_m \geq 1$). Thus, despite the possibility of extensive reconnection, it is unlikely that the solar wind drives a large-scale convection system. Two very different models have been proposed for the internal dynamics of Uranus' magnetopshere. Hill et al.(1983) assumed the absence of a strong internal source of plasma and suggested that the rotating ionosphere is electrodynamically coupled to the solar wind by field-aligned (Birkeland) currents in a manner analogous to a Faraday disc dynamo. With the ionosphere acting as the disc dynamo the currents transfer planetary rotational energy and angular momentum to the magnetosheath. Thus the magnetosheath plasma flow would be helical under the combined influences of the solar wind and the planetary rotation. From their analytical model of the disc dynamo Hill et al.(1983) calculated that the particles carrying the Birkeland currents into the ionosphere could readily provide enough power to account for the observed auroral emission.

An alternative model has been proposed by Cheng(1984) who predicts that the Uranian magnetosphere will be dominated by satellite plasma sources and internally-driven convection, on a scale similar to that of Saturn's magnetosphere. Cheng(1984) points out that there are four icy satellites within 22.6 $R_U$ that are comparable in size with Rhea, Dione and Tethys, the main sources of plasma in Saturn's magnetosphere. Cheng(1984) argues that charged-particle sputtering of these icy satellites could provide a comparable plasma population in Uranus' magnetosphere. The crucial issue is whether the charged-particle mechanism can be self-generating or whether a seed population of energetic particles, either from another internal source (such as the dense atmosphere of Titan in Saturn's case) or from the solar wind, is necessary.

### 9.2.8 Neptune and Pluto

Delving further into the realms of speculation we turn to the two outermost planets of the solar system. Neptune is very similar to Uranus though its rotation axis has the more usual orientation, perpendicular to the ecliptic. If Neptune has a substantial magnetic field then it is possible that Neptune's large satellite Triton ($R \geq 1500$ km) is embedded in the planet's magnetosphere, and with an atmosphere it could play a similar role to Titan in Saturn's magnetosphere. If all goes to plan, Voyager 2 will visit Neptune in 1989, first passing very close ($0.4\ R_N$) over the north pole of the planet and then passing close to Triton.

No bigger than the Moon, Pluto ($1300 \leq R_P \leq 2000$ km) and its satellite Charon may have escaped from orbit around Neptune and barely qualify as a separate planetary system. Although it seems unlikely that Pluto would have an intrinsic magnetic field, even a weak field would carve a relatively large magnetopsheric cavity in the very tenuous ($n_{sw} \approx 5 \times 10^{-3}$ particles $cm^{-3}$) solar wind at 39 A.U.

## 9.3 CONCLUSIONS

In this chapter I have attempted to outline our understanding of the plasma environments around various planetary bodies. Considering planetary magnetospheres as a family of related objects one looks for underlying physical principles which allow comparison between them, ranging from the small cavity around Mercury to the giant magnetosphere of Jupiter. For example, a major factor governing magnetospheric structure and plasma dynamics is the relative importance of (internal) forces derived from planetary rotation compared with (external) forces driven by the solar wind. It is also important to consider the various particle populations in different regions of the magnetospheres, their origins (i.e. the solar wind, planetary ionospheres or satellites embedded in the magnetospheric plasma) and how they produce phenomena such as plasma waves, aurorae, radio emissions, etc., which are common to planetary magnetospheres. These studies can be extended to include the interaction regions surrounding unmagnetised bodies immersed in a plasma flow such as Venus, a planet with a deep atmosphere sitting in the supersonic solar wind, or Io, a satellite orbitting in the transsonic flow of magnetospheric plasma. To date, the magnetospheres of six planets have been explored directly with spacecraft carrying different selections of instruments to measure electric and magnetic fields plus particle detectors covering a wide range of energies. Some of the planetary magnetospheres have also been observed remotely from the Earth via their electromagnetic emissions ranging from X-ray to radio wavelengths. It is clear that comparative studies are in their infancy and we are likely to see them develop considerably over the next decade as spacecraft further explore the solar system.

from lengthy discussions with colleagues in the space plasma groups at M.I.T. and Imperial College. In particular I am indebted to Ralph McNutt and David Southwood. I would like to thank John Richardson and Mark Saunders for giving material before publication. I am also grateful to Hilary Todd for her assistance with the manuscript.

REFERENCES

Bagenal F & J D Sullivan (1981) *J. Geophys. Res.* 86, 8447.
Bagenal F (1983) *J. Geophys. Res.* 88, 3013.
Bagenal F (1985) *J. Geophys. Res.* 90, 311.
Bagenal F, R L McNutt, J W Belcher, H S Bridge & J D Sullivan (1985) *J. Geophys. Res.* 90, 1755.
Belcher J W, C K Geortz, J D Sullivan & M H Acuna (1981) *Geophys. Res. Lett.* 86, 8508.
Belcher J W (1983) in Dessler(1983).
Biermann L (1957) *Observatory* 77, 109.
Bigg E K (1964) *Nature* 203, 1008.
Brice N M & G A Ionnidis (1970) *Icarus* 13, 173.
Bridge H S, J W Belcher, A J Lazarus, S Olbert, J D Sullivan, F Bagenal, P Garzis, R H Hartle, K W Ogilvie, J D Scudder, E C Sittler, A Eviatar, G L Siscoe, C K Goertz, V M Vasyliunas (1981) *Science* 212, 217.
Broadfoot A L, B R Sandel, D E Shemansky, J B Holberg, G R Smith, D F Strobel, J C McConnell, S Kumar, D M Hunten, S K Atreya, T M Donahue, H W Moos, J L Bertaux, J E Blamont, R B Pomphrey, S Linick (1981) *Science* 212, 206.
Brown R A (1974) *Exploration of the planetary system*, ed. A Woszczyk & C Iwaniszewska, D.Reidel.
Brown R A (1976) *Astrophys. J.* 206, L179.
Brown R A (1981) *Astrophys. J.* 244, 1072.
Brown R A, C B Pilcher & D F Strobel (1983) in Dessler(1983).
Burke B F & K L Franklin (1955) *J. Geophys. Res.* 60, 213.
Chapman S & V C A Ferraro (1931) *Terr. Magn. Atmos. Elect.* 36, 77.
Cheng A F (1984) *Workshop on Uranus and Neptune* ed. J T Bergstrahl, NASA conference publication 2330.
Clarke J T (1982) *Astrophys. J.* 263, L105.
Dessler A J (1983) *Physics of the Jovian magnetosphere*, Cambridge University Press.
Dolginov Sh Sh (1978) *Geophys. Res. Lett.* 5, 93.
Dungey J W (1965) *Space Sci. Rev.* 4, 199.
Durrance S T & H W Moos (1982) *Nature* 299, 428.
Durrance S T, P D Feldman & H A Weaver (1983) *Astrophys. J.* 267, L125
Gehrels T & M S Mathews (1984) *Saturn*, U Arizona Press, Tucson, Arizona.
Gledhill J A (1967) *Nature* 214, 155.
Gold T (1959) *J. Geophys. Res.* 64, 1219.
Goldreich P & D Lynden-Bell (1969) *Astrophys. J.* 156, 59
Goertz C K & P A Deift (1973) *Planet. Space Sci.* 21, 1399.

Goertz C K (1980) *J. Geophys. Res.* 85, 2949.
Gurnett D A (1972) *Astrophys. J.* 175, 525.
Gurnett D A & C K Goertz (1981) *J. Geophys. Res.* 86, 717.
Hill T W, A J Dessler & F C Michel (1974) *Geophys. Res. Lett.* 1, 3.
Hill T W & F C Michel (1975) *Rev. Geophys. & Space Phys.* 13, 967.
Hill T W, A J Dessler & M E Rassbach (1983) *Planet. Space Sci.* 31, 1187.
Kupo I , Y Mekler & A Eviatar (1976) *Astrophys. J.* 205, L51.
Lazarus A J & R L McNutt (1983) *J. Geophys. Res.* 88, 8831.
Marshall L & W F Libby (1967) *Nature* 214, 126.
McNutt R L (1983) *Adv. Space Res.* 3, 55.
McNutt R L (1984) *Magnetospheres in the solar system,* European Space Agency report ESA SP-207.
Melrose D B (1967) *Planet. Space Sci.* 15, 381.
Ness N F (1979) *Solar system plasma physics,* III, ed. C F Kennel, L J Lanzarotti & E N Parker, North-Holland.
Neubauer F M (1980) *J. Geophys. Res.* 85, 1171.
Neubauer F M, D A Gurnett, J D Scudder & R E Hartle (1984) in Gehrels and Matthews(1984)
Neugebauer M & C W Snyder (1962) *Science* 138, 1095.
Phillips J L, J G Luhmann & C T Russell (1984) *J. Geophys. Res.* 89,10676.
Piddington J H & J F Drake (1968) *Nature* 217, 925.
Richardson J D & G L Siscoe (1981) *J. Geophys. Res.* 86, 8485.
Richardson J D & G L Siscoe (1983) *J. Geophys. Res.* 88, 2001.
Richardson J D (1985) *J. Geophys. Res.* in press.
Russell C T (1978) *Geophys. Res. Lett.* 5, 85.
Russell C T & R C Elphic (1979) *Nature* 279, 616.
Russell C T, R C Elphic & J A Slavin (1980) *J. Geophys. Res.* 85, 8319.
Russell C T, J G Luhmann, R C Elphic & M Naugebauer (1982) *Comets* ed. L L Wilkening, U Arizona Press.
Russell C T, J G Luhmann, J R Spreiter & S S Stahara (1984) *J. Geophys. Res.* 89, 2997.
Saunders M A & C T Russell (1985) *J. Geophys. Res.* in press.
Schardt A W, K W Behannon, R P Lepping, J F Carbary, A Eviatar, G L Siscoe (1984) in Gehrels and Matthews(1984).
Sittler E C, K W Ogilvie & J D Scudder (1983) *J. Geophys. Res.* 88, 8847.
Siscoe G L (1971) *Planet. Space Sci.* 19, 483.
Siscoe G L (1975) *Icarus* 24, 311.
Siscoe G L (1979) *Solar system plasma physics,* III ed. C F Kennel, L J Lanzarotti & E N Parker, North-Holland.
Siscoe G L & L Christopher (1975) *Geophys. Res. Lett.* 2, 158.
Siscoe G L, N F Ness & C M Yeates (1975) *J. Geophys. Res.* 80, 4359.
Siscoe G L & D Summers (1981) *J. Geophys. Res.* 86, 8471.
Slavin J A & R E Holzer (1982) *J. Geophys. Res.* 87, 10285.
Sonnerup B U O & M J Laird (1963) *J. Geophys. Res.* 68, 131.
Southwood D J, M G Kivelson, R J Walker & J A Slavin (1980) *J. Geophys. Res.* 85, 5959.
Spreiter J R, M C Marsh & A L Summers(1970) *Cosmic Electrodynamics* 1, 5.

Stern D P & N F Ness (1982) *Ann. Rev. Astron. Astrophys.* 20, 139.
Taylor H E, K W Behannon & N F Ness (1968) *J. Geophys. Res.* 73, 6763.
Vasyliunas V M (1983a) *Solar-terrestrial Physics* ed. R L Carovillano & J M Forbes, D Reidel.
Vasyliunas V M (1983b) in Dessler(1983).